

Full Length Research Paper

Structural, magnetic and transport properties of samarium (Sm) doped Cu-Zn ferrites

Prodip Kumar Mondal¹, Mohammad Alamgir Hossain^{1*}, Mohammed Nazrul Islam Khan² and Shibendra Shekher Sikder¹

¹Department of Physics, Khulna University of Engineering and Technology, Khulna-9203, Bangladesh.

²Materials Science Division, Atomic Energy Center, Dhaka 1000, Bangladesh.

Received 29 June, 2018; Accepted 20 August, 2018

The present work is focused on investigating the effect of rare earth ion on structural, magnetic and transport properties of $(\text{Cu}_{0.5}\text{Zn}_{0.5}\text{Fe}_{2-x})\text{Sm}_x\text{O}_4$ [$x = 0.00, 0.05$ and 0.10] ferrites which were prepared by solid state reaction technique at 1100°C for 3 h. The X-ray diffraction analysis revealed that rare earth free sample shows formulation of single phase cubic spinel structure with no extra peak whereas Sm substituted Cu-Zn ferrite samples show additional peaks that correspond to a secondary orthoferrite phase. Lattice parameter, bulk density, X-ray density and porosity of the studied samples are increased with Sm substituted ions. Lattice parameter of both series are slightly decrease with increase Sm content. The initial permeability decreases with increasing Sm ions in ferrite. Quality factor signifies the merit of the material from the application point of view. The dielectric constant was found to decrease continuously with increasing frequency and remain almost constant at higher frequency range. The dielectric behavior of the experimental ferrite samples can be explained on the basis of the mechanism of the dielectric polarization and conduction process. The saturation magnetization decreases with increasing rare earth Sm contents.

Key words: Solid state reaction technique, sintering temperature, quality factor, dielectric polarization.

INTRODUCTION

Rare earth oxides are recently becoming the promising and potential additives for the improvement of the properties of ferrites. Physical, electrical and magnetic properties arise from the ability of the ferrites to distribute the cations among the available A and B sites, and the relative strengths of exchange interactions. The properties can be changed by substitutions with various kinds of divalent cations or relatively small amount of rare earth ions. Many researchers reported on the influence of different additions and substitutions on structural, electrical and magnetic properties of ferrites (Costa et al., 2003; Mohamed et al., 2003; Calderon-Qritiz et al., 2007; Hossain et al., 2015). Recently enormous studies are

conducted on rare earth ferrites (Hossain et al., 2018; Hussain and Rusul, 2018; Qindeela and Alonizan, 2018; Das and Prasad, 2016; Heiba et al., 2017). Some properties are very much sensitive to preparation environment such as sintering temperature, time and type of additives. Present study demonstrates that the addition of small amount of rare earth ions to Cu-Zn ferrite samples produces a change in their structural, magnetic and electrical properties depending upon the type and the amount of rare earth elements used.

Rare earth element has large magnetic moments, large magnetocrystalline anisotropy and very large magnetostriction at low temperature due to their localized

*Corresponding author. E-mail: liton@phy.kuet.ac.bd.

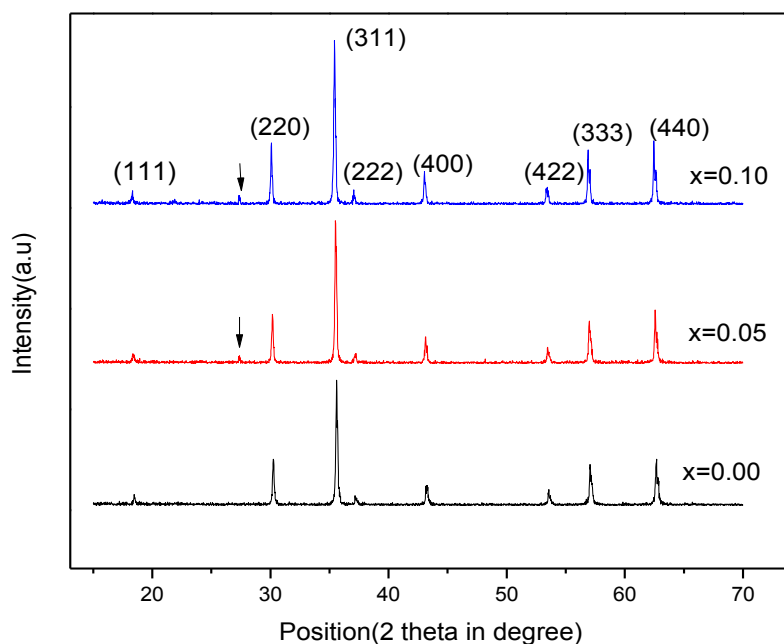


Figure 1. X-ray diffraction patterns of $(\text{Cu}_{0.5}\text{Zn}_{0.5}\text{Fe}_{2-x})\text{Sm}_x\text{O}_4$ [$x = 0.05, 0.10$] ferrites sintered at 1100°C for 3 h.

nature of 4f electrons being totally screened by 5s and 5p orbital (Ben et al., 2008; Mansour, 2000). The substitution of ferrite ions by rare earth Sm ions shows the over flow of the sub lattice B site and enter in to the grain boundaries which makes the secondary phase known as orthoferrite phase (Nutan et al., 2007). Substitution of rare earth for Fe^{3+} in the octahedral site may show some interesting electromagnetic properties. Structural characterization and identification of phases is a priority for the study of ferrites. The structural, magnetic and electrical properties of various polycrystalline of $\text{Cu}_{0.5}\text{Zn}_{0.5}\text{Fe}_{2-x}\text{Sm}_x\text{O}_4$ ferrites where $x = 0.00, 0.05, 0.10$ ferrites are studied. Samples are prepared with solid state reaction method and sintered at temperature 1100°C for 3 h. Optimum structural, electrical and magnetic properties of the ferrites necessitate have been investigated with variation Fe-deficient in Cu-Zn ferrites. The magneto transport properties are discussed for different concentration of Sm substitution on Cu-Zn ferrite. The effects of Sm^{3+} substitution on the density, permeability, magnetic loss, saturation magnetization and dielectric constant of Cu-Zn-RE ferrites.

METHODOLOGY

The ferrites of different compositions were prepared using ceramic technique involving solid state reaction from metal oxides (CuO , ZnO , La_2O_3 , Sm_2O_3 and Fe_2O_3) in the form of grained powder having 99.95% purity. Different oxides were weighed precisely according to their molecular weight. The weight percentage of the various oxides was mixed. The slurry prepared in is dried, palletized and then transferred to a porcelain crucible for pre sintering in a constant temperature of 1000°C for 4 h. Presintering of the materials

was performed in a furnace named Gallen Kamp at AECD (Atomic Energy Centre, Dhaka). The cooling and heating rates were $4^\circ\text{C}/\text{min}$. These oxide mixtures were milled thoroughly for 4 to 6 h to obtain homogeneous mixture. The mixture was dried and a small amount of saturated solution of polyvinyl alcohol (PVA) were added as a binder and pressed into pellet and toroid shape respectively under pressure 1.75 and $1.2 \text{ ton}\cdot\text{cm}^{-2}$ using hydraulic press. The prepared samples were sintered at 1100°C for 3 h with a microprocessor controlled muffle furnace. The samples were polished in order to remove any oxide layer formed during the process of sintering. Thus the final specimens were obtained.

RESULTS

X-ray diffraction analysis

X-ray diffraction analysis is a useful technique to evaluate the various phases of the synthesized ferrites as well as their unit cell parameters. In the present study, X-ray diffraction (XRD) studies of the samples were performed by using Philips PERT PRO X-ray diffraction using $\text{Cu}\text{-K}\alpha$ radiation in the range of $2\theta = 20^\circ$ to 70° in steps of 0.02° .

The phase formation behavior of $\text{Cu}_{0.5}\text{Zn}_{0.5}\text{Fe}_2\text{O}_4$ ferrite sintered at 1100°C for 3 h are studied. All samples show good crystallization with well-defined diffraction lines. The XRD patterns for all the samples were indexed for fcc spinel structure and the Bragg planes are shown in the patterns. The peaks (111), (220), (311), (222), (400), (422), (333) and (440), indicating that the samples are corresponding to spinel phase with a single phase. The samples have been characterized as cubic spinel structure without any extra peaks corresponding to any secondary phase (Figure 1).

Table 1. Data of the lattice parameter (a), X-ray density (d_x), bulk density (d_B) of $(\text{Cu}_{0.5}\text{Zn}_{0.5}\text{Fe}_{2-x})\text{Sm}_x\text{O}_4$ ($x=0.00, 0.05$ and 0.10) ferrites sintered at 1100°C for 3 h.

Sample composition	$a_o(\text{Å})$	$d_x(\text{gm/cm}^3)$	$d_B(\text{gm/cm}^3)$	Porosity%
$\text{Cu}_{0.5}\text{Zn}_{0.5}\text{Fe}_2\text{O}_4$	8.368	5.45	4.35	20.18
$(\text{Cu}_{0.5}\text{Zn}_{0.5}\text{Fe}_{1.95})\text{Sm}_{0.05}\text{O}_4$	8.362	5.33	4.57	14.25
$(\text{Cu}_{0.5}\text{Zn}_{0.5}\text{Fe}_{1.9})\text{Sm}_{0.1}\text{O}_4$	8.358	5.32	4.52	15.03

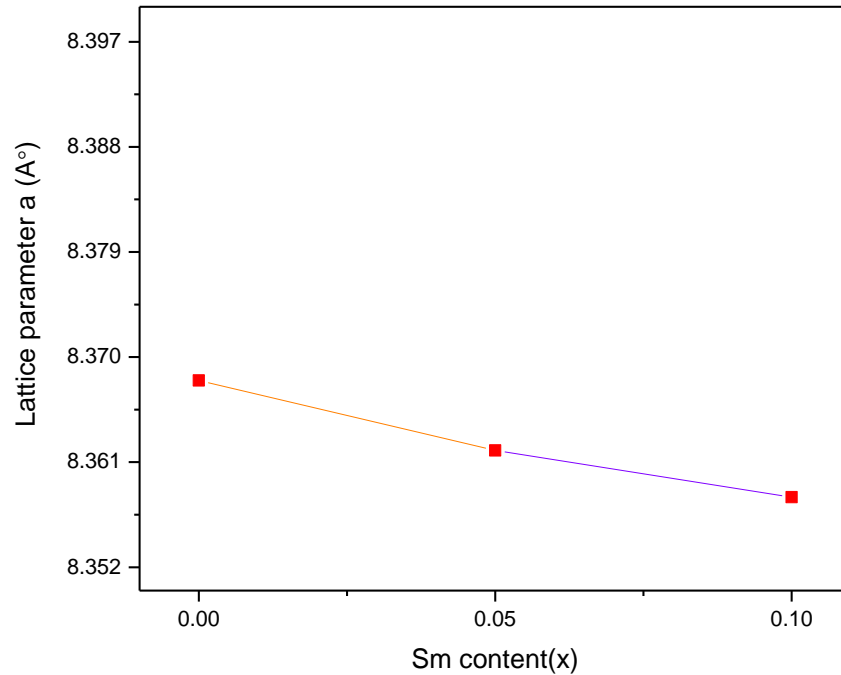


Figure 2. Lattice parameters calculated from X-ray diffraction patterns plotted as a function of Sm content in the series $(\text{Cu}_{0.5}\text{Zn}_{0.5}\text{Fe}_{2-x})\text{Sm}_x\text{O}_4$

Lattice parameters

The values of the lattice parameters has been obtained from each plane are plotted against Nelson-Riley function

(Nutan et al., 2007). $F(\theta) = \frac{1}{2} \left[\frac{\cos^2\theta}{\sin\theta} + \frac{\cos^2\theta}{\theta} \right]$, where θ

is the Bragg's angle by extrapolating lattice parameter's value of $F(\theta) = 0$ or 90° . Table 1 shows the exact lattice parameters. Figure 2 shows the relation between lattice parameters of Samarium contents in Cu-Zn ferrites.

Density and porosity

The bulk density (d_B) was measured by usual mass and dimensional consideration whereas X-ray density (d_x) was calculated from the molecular weight and the volume of the unit cell for each sample by using the Equations 1

and 2.

$$d_B = \frac{m}{V} = \frac{m}{\pi r^2 h} \quad (1)$$

$$d_x = \frac{8M}{Na^3} \text{ gm/cm}^3 \quad (2)$$

The calculated values of the bulk density and theoretical (or X-ray) density of the present ferrite system are listed in Table1 for Sm substituted in Cu-Zn ferrites.

Frequency dependence of complex permeability

The complex permeability is given by $\mu = \mu' - i\mu''$, μ' is the real permeability (in phase) and μ'' the

imaginary permeability (90° out of phase). Complex permeability has been determined as a function of frequency up to 120 MHz at room temperature for all the samples of series $(\text{Cu}_{0.5}\text{Zn}_{0.5}\text{Fe}_{2-x})\text{Sm}_x\text{O}_4$ [$x = 0.00, 0.05, 0.10$] ferrites by using the conventional technique based on the determination of the complex impedance of circuit loaded with toroid shaped sample.

Frequency dependence of complex initial permeability Sm substituted Cu-Zn ferrites

The optimization of the dynamic properties such as complex permeability in the high frequency range requires a precise knowledge of the magnetization mechanisms involved. From Figure 4 it is noticed that the real component of permeability, μ' is fairly constant with frequency up to certain high frequency range, and then falls slowly value at maximum frequency. It is clearly evident from this figure that the initial permeability as a function of frequency in the range high MHz range and with decreases initial permeability with increase Sm content x monotonically (Figure 5).

Frequency dependence of quality factor

The frequency dependence of $(\text{Cu}_{0.5}\text{Zn}_{0.5}\text{Fe}_{2-x})\text{Sm}_x\text{O}_4$ (Sm and $x = 0.00, 0.05, 0.10$) ferrites sintered at temperature at 1100°C for 3 h have been calculated from the relation $Q = 1/\tan\delta$; where $\tan\delta$ is the loss factor is used to measure the merit of the magnetic materials. Figure 6 shows the frequency dependence quality factors (Q-factors) of sample $(\text{Cu}_{0.5}\text{Zn}_{0.5}\text{Fe}_{2-x})\text{Sm}_x\text{O}_4$ sintered at temperature at 1100°C for 3 h. Q-factor increases with an increase of frequency showing a maximum value. The variation of the relative quality factor with frequency showed a similar trend for all the samples. Q-factor increases with increases of frequency showing no peak and peak must be may be > 120 MHz range.

Field dependence of magnetization of Sm substituted Cu-Zn ferrites

Figure 7 shows the M_s values or saturate level of Sm substituted ferrites is lower than that of unsubstituted specimen. This might be due to a better bulk density and a decrease in permeability with increasing Sm substitution.

Frequency dependence of dielectric constant

Figure 8 shows the variation of dielectric constant, ϵ' with frequency for different composition of $(\text{Cu}_{0.5}\text{Zn}_{0.5}\text{Fe}_{2-x})\text{Sm}_x\text{O}_4$ where $x = 0.00, 0.05, 0.10$ ferrites sintered at 1100°C for 3 h, 1 to 120 MHz at room temperature. It can

be seen from the figure that the dielectric constant is found to decrease continuously with increasing frequency for all the specimens exhibiting a normal dielectric behavior of ferrites.

DISCUSSION

The Sm substituted $(\text{Cu}_{0.5}\text{Zn}_{0.5}\text{Fe}_{2-x})\text{Sm}_x\text{O}_4$ ferrites where $x = 0.00, 0.05, 0.10$ sintered at 1100°C for 3 h were studied by XRD. Figure 1 shows the XRD patterns of the as-burnt ferrite powders. The phase analysis revealed that the as burnt ferrite powders were crystalline in nature and the peaks (220), (311), (222), (400), (422), (333) and (440) correspond to spinel phase structures with a single phase. The lattice parameter 'a' corresponding to each plane was calculated by using the X-ray data. With the substitution of rare earth Sm into Cu-Zn Ferrite an extra peak SmFeO_3 is found. The peak intensity is increased with increasing Sm concentration. This apparently indicated that the Sm did not form a solid solution with spinel ferrites or it had very small solid solubility. Table 1 shows the lattice parameters, bulk density, theoretical density and apparent porosity. Table 1 shown in a marginal decrease in 'a₀' of $(\text{Cu}_{0.5}\text{Zn}_{0.5}\text{Fe}_{2-x})\text{Sm}_x\text{O}_4$ ferrite with Sm substitution, which might be due to the compressive pressure exerted on the ferrite lattice by SmFeO_3 . There is a slight decrease Sm^{3+} (radius = 1.09\AA) in the octahedral sites, indeed, lattice parameter was in the same range of different. This decrease can be attributed to the vacancy created by Zn^{2+} deficiencies with increasing its Sm^{3+} content. The unit cell is expected to reduce size by contraction of the lattice resulting in decrease of lattice parameter gradually.

The X-ray density decreases continuously with increasing Sm content as shown in Figure 3. This may be due to the existence of pores which were formed and developed during the sample preparation or sintering process. The bulk density initially increases with increasing rare earth ions Sm^{3+} finally minor decrease in with increase Sm substitution. It may be also be mentioned that reduction Fe^{2+} due to Fe^{3+} deficiency is expected to increase the resistivity of the samples. This density plays an important role on the magnetic properties. Table 1 shows the results of lattice parameter, theoretical density, and bulk density calculated porosity for Sm doped Cu-Zn ferrites. The enhancement of Bulk density is due to activated diffusion process triggered by the excess vacancies created by Zn^{2+} deficiency. Specimens contained some closed porosity. It was difficult to remove these closed porosities completely due to the evaporation of constituents specially Zn. The intergranular porosity mainly depends on the grain size. At higher sintering temperatures, the density is decreased because the intragranular porosity is increased resulting from discontinuous grain growth.

It is well established that permeability of polycrystalline

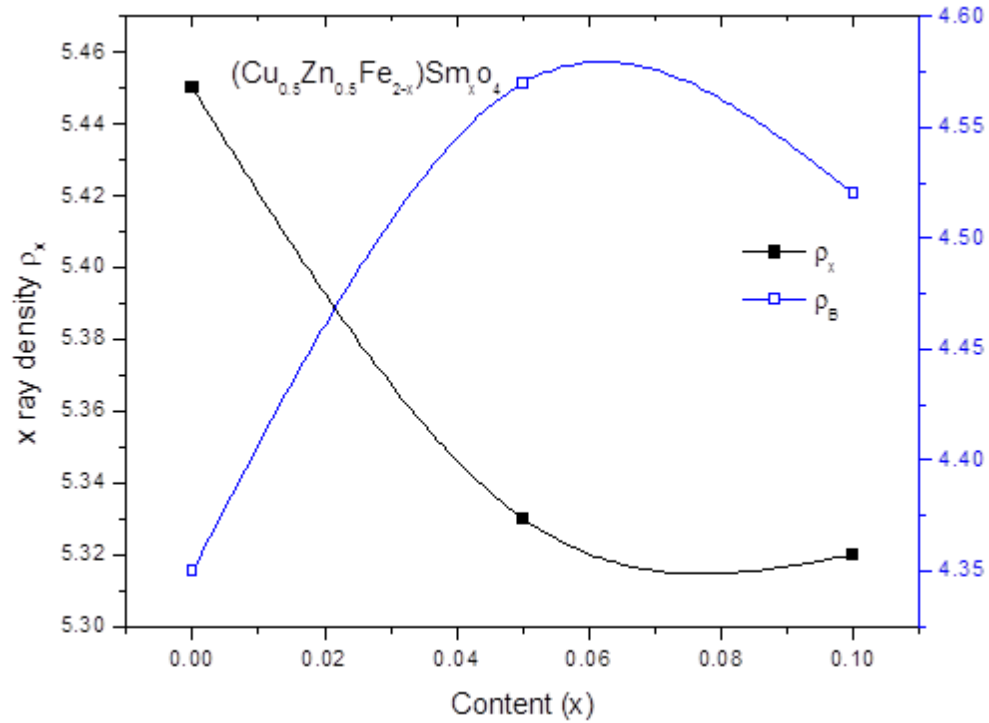


Figure 3. Variation of bulk density and X-ray density as a function of Sm content.

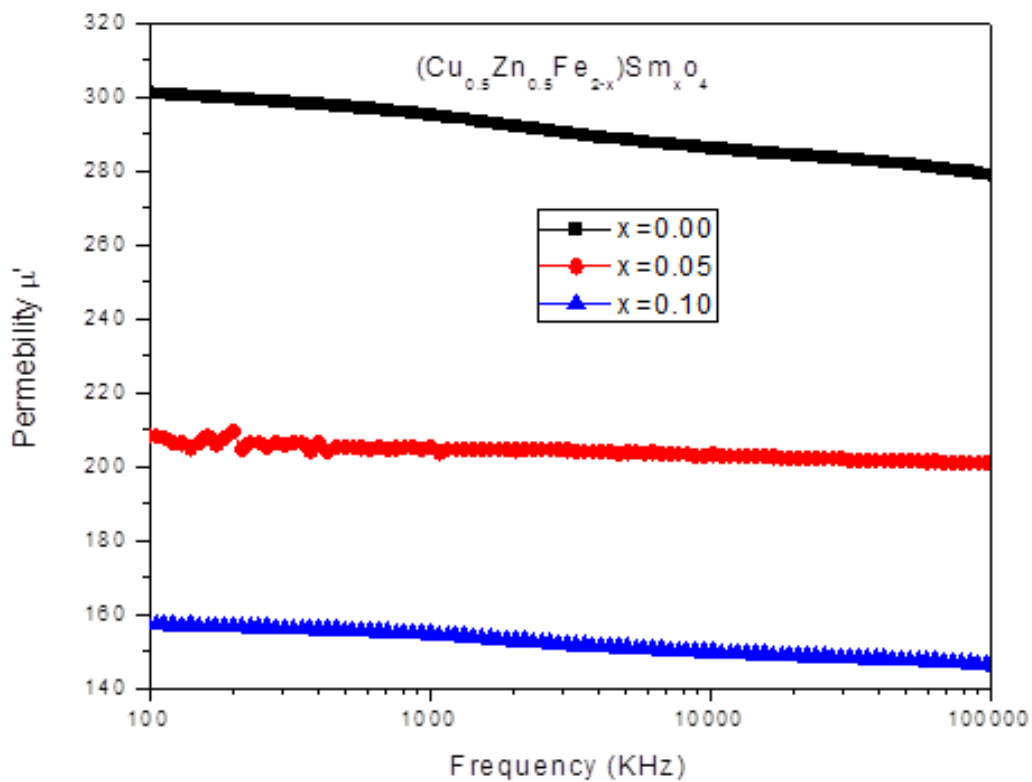


Figure 4. Variation of real part of initial permeability as a function of $(\text{Cu}_{0.5}\text{Zn}_{0.5}\text{Fe}_{2-x})\text{Sm}_x\text{O}_4$ where $x = 0.00, 0.05, 0.10$ sintered at 1100°C for 3 h.

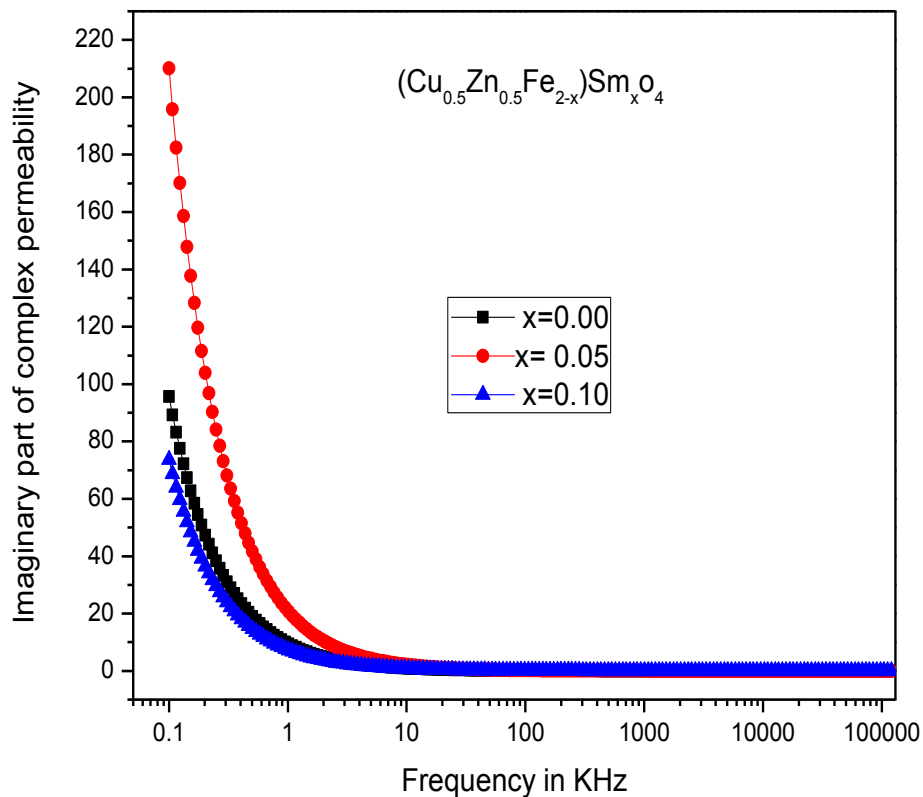


Figure 5. Variation of Complex imaginary permeability μ'' as a function of $(\text{Cu}_{0.5}\text{Zn}_{0.5}\text{Fe}_{2-x})\text{Sm}_x\text{O}_4$ where $x = 0.00, 0.05, 0.10$ sintered at 1100°C for 3 h.

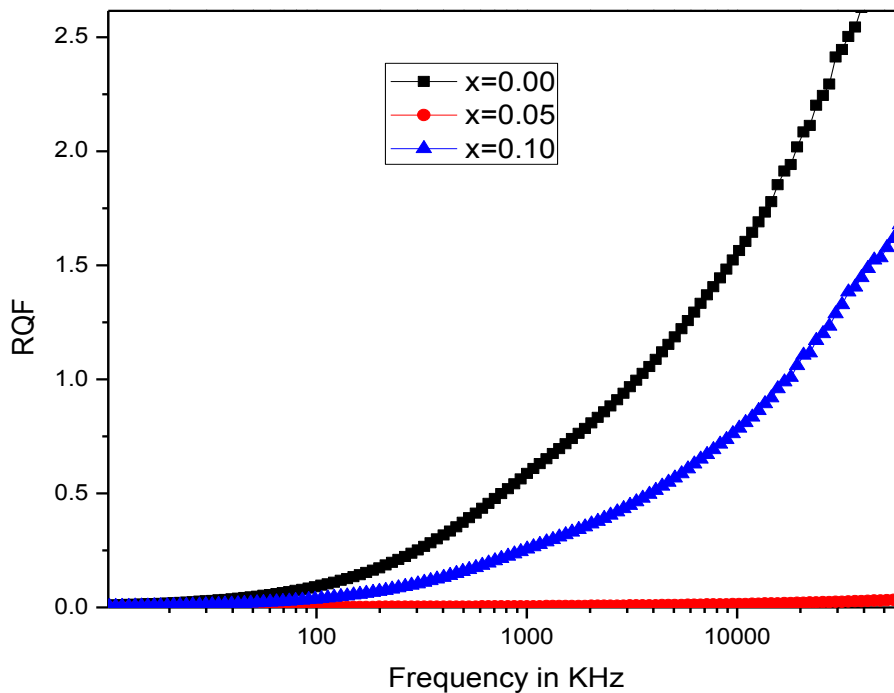


Figure 6. Variation of relative quality factor (RQF) as a function of $(\text{Cu}_{0.5}\text{Zn}_{0.5}\text{Fe}_{2-x})\text{Sm}_x\text{O}_4$ where $x = 0.00, 0.05, 0.10$ sintered at 1100°C for 3 h.

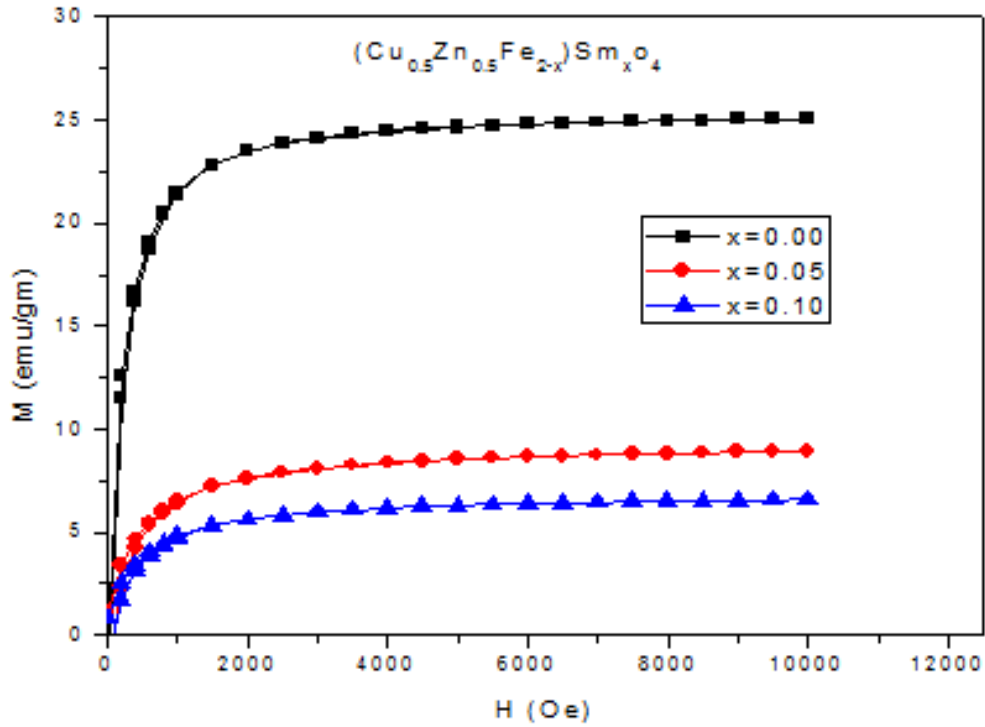


Figure 7. Variation of magnetization at room temperature as a function of applied field on $(\text{Cu}_{0.5}\text{Zn}_{0.5}\text{Fe}_{2-x})\text{Sm}_x\text{O}_4$ where $x = 0.00, 0.05, 0.10$ sintered at 1100°C for 3 h.

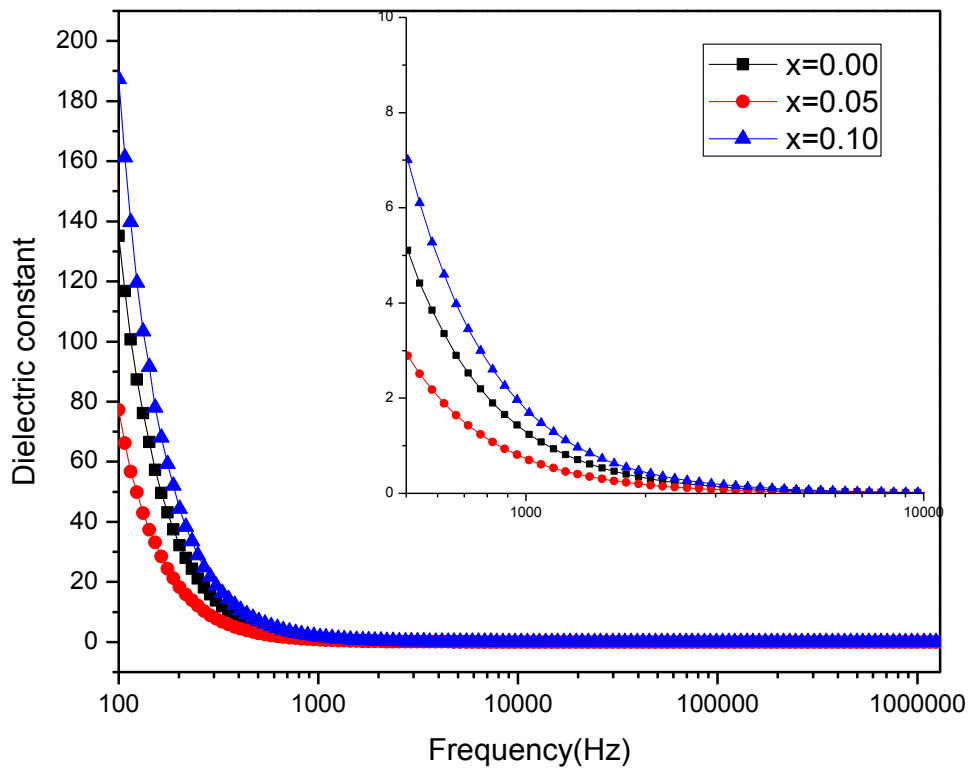


Figure 8. Variation Dielectric constant at room temperature as a function of frequency of the ferrite system on $(\text{Cu}_{0.5}\text{Zn}_{0.5}\text{Fe}_{2-x})\text{Sm}_x\text{O}_4$ where $x = 0.00, 0.05, 0.10$ sintered at 1100°C for 3 h.

ferrite increases with increasing density and grain size. Decrease in permeability with Sm substitution might primarily be attributed to the increase in bulk density. An increase in the density, not only results in the reduction of demagnetizing field due to the reduction of pores but also raises the spin rotational contribution, which turns decrease the permeability.

Figure 5 shows the imaginary part of complex permeability first rises and suddenly decreases at low value at constant up to high frequency MHz range of are stable ($\text{Cu}_{0.5}\text{Zn}_{0.5}\text{Fe}_{2-x}\text{Sm}_x\text{O}_4$) ferrites. When frequency is low, imaginary permeability is high and when frequency is high imaginary permeability is low. Thus an effective limit of product of frequency and imaginary permeability is established. So that effect of rare earth content of high frequency and high imaginary permeability are mutually incompatible.

Figure 7 shows the decrement of saturation of magnetization. This has due to the presence of higher quantity of nonmagnetic SmFeO_3 phase. The decrease M_s seems that strong short range ferromagnetic ordering and frustration coexists with in the antiferromagnetic matrix. The observed decrease magnetization curves are mentioned of each composition on the distribution of Fe^{3+} ions between the two sublattices A and B, where the Zn^{2+} and Cu^{2+} and Sm^{3+} ions are nonmagnetic. Hence the present system Sm substituted Cu-Zn ferrites, frustration and randomness decreases in M_s shows significant departure from Nell's collinear model. The dielectric dispersion is rapid at lower frequency region and it remains almost independent at high frequency side. The incorporation of rare earth element Sm in Figure 8 into these ferrites has no pronounced effect on the dielectric constant in high frequency, but significantly decreases the dielectric constant in the low frequency range.

The magnitude of exchange depends on the concentration $\text{Fe}^{2+}/\text{Fe}^{3+}$ in pairs present on B-site for the present ferrite. This could be explained using Koop's phonological theory (Maxwell, 1873), which has based on the Maxwell-Wagner model (Maxwell, 1873; Reddy and Rao, 1982) for inhomogeneous double layer dielectric structure. The dielectric structure has supposed to be composed of the fairly well conducting ferrite grains. The first layer is the fairly well conducting large ferrite grain which is separated by the second thin layer of the poorly conducting grain boundaries. The grain boundaries of the lower conductivity were found to be ferrite at lower frequencies while ferrite grains of high conductivity are effective at high frequency.

Conclusion

The substitution of Sm for in ($\text{Cu}_{0.5}\text{Zn}_{0.5}\text{Fe}_{2-x}\text{Sm}_x\text{O}_4$) ferrites revealed mainly the formation of secondary phase of composition SmFeO_3 . The lattice parameter decreases with increasing Sm contents obeying Vagard's law. Bulk density of the ferrites increased with increasing Sm substitution, increased densification might be due to the

appearance of excess Cu and Zn compared to Fe in the composition with respect Sm content.

The initial permeability decreases with increasing Sm substituted Cu-Zn ferrites monotonically. Decrease in permeability with Sm substitution might primarily be attributed to the increase in bulk density and may be due to secondary phase of SmFeO_3 segregated in the prepared samples. The imaginary permeability initially rises and suddenly decreases at low value at constant up to high frequency in MHz range.

Magnetization increases sharply at very low field ($H < 1\text{kOe}$) which corresponds to magnetic domain reorientation due to domain wall displacement and there after increase slowly up to saturation due to spin rotation for both rare earth Sm substituted Fe in Cu-Zn ferrites. The magnetization process is connected with soft magnetic behavior of magnetic material. Saturation magnetization decreases with increasing Sm substituted Fe in Cu-Zn ferrites can be explained on the basis of cation distribution and exchange interaction on A- and B-sites. The saturated value of magnetization is lower of Sm substituted Cu-Zn ferrite than the value of magnetization of unsubstituted one. This indicates the strong short range ferromagnetic ordering and frustration coexists with in the antiferromagnetic matrix. Normally, the dielectric constant decreases with increasing frequency. This phenomenon is shown for all samples. Maximum dielectric is found for the sample $x=0.10$. The increases in frequency enhance the hopping frequency of charge carriers, resulting in an increase in the conduction process, thereby decreasing the dielectric constant. Dielectric structure to be composed of the fairly well conducting ferrite grain.

The loss is due to lag of domain wall motion with respect to the applied alternating magnetic field and is attributed to various domain defects (Shrotri et al., 1999) which include non-uniform and non-repetitive domain wall motion, domain wall bowing, localized variation of flux density, nucleation and annihilation of domain walls. This phenomenon is associated with the ferromagnetic resonance within the domains (Shrotri et al., 1999) and at the resonance maximum energy is transferred from the applied magnetic field to the lattice resulting in the rapid decreases in RQF. Cu-Zn-La, Cu-Zn-Sm ferrites have been found to demonstrate reasonably good permeability at room temperature covering stable wide range of frequency indicating the possibilities for applications as high frequency up to several MHz induction and/or core materials. The corresponding to maxima Q-factor shifts to lower frequency range as increase of La or Sm content.

CONFLICT OF INTERESTS

The authors have not declared any conflict of interests.

ACKNOWLEDGEMENTS

Prof. S. S. Sikder is thankful to Khulna University of

Engineering and Technology (KUET) for providing fund to conduct this research work, Moreover, one of the authors (M. A. Hossain) is thankful to the Materials Science Division of Atomic Energy Centre, Dhaka (AECDC), Bangladesh for utilizing the laboratory facilities for various measurements.

REFERENCES

- Costa ACM, Morelli MR, Kiminami RHGA (2003). Microstructure and Magnetic properties of Ni-Zn-Sm ferrites", *Ceramica* 49:168.
- Mohamed O, Hemeda MM, Barbka MM, Hemeda DM (2003). Structural, electrical and spectral studies on rare earth orthoferrites $\text{La}_{1-x}\text{Nd}_x\text{Fe}_2\text{O}_3$ ", *Turkish Journal of Physics* 27:537.
- Calderon-Qrutz E, Perales-Perez O, Voyles P, Guterrez G, Tomar MS (2007). $\text{Mn}_x\text{Zn}_{1-x}\text{Fe}_{2-y}\text{R}_y\text{O}_4$ (R = Gd, Eu) ferrites nanocrystals for potential magnetocaloric application, [in] ENS'07, Paris.
- Hossain MA, Khan MNI, Sikder SS (2015). Effect of Resistivity, Permeability and Curie Temperature of Rare Earth Metal Europium (Eu) Substitution on $\text{Ni}_{0.60}\text{Zn}_{0.40-x}\text{Eu}_x\text{Fe}_2\text{O}_4$ (x = 0.05, 0.10, 0.15) Ferrites. *ARPN Journal of Science and Technology* 5(10):520-524.
- Hossain MA, Khan MNI, Sikder SS (2015). Study of the Variation of Resistivity, Permeability and Curie Temperature of Rare Earth Metal lanthanum (La) Substitution on $\text{Ni}_{0.60}\text{Zn}_{0.40-x}\text{La}_x\text{Fe}_2\text{O}_4$ (x=0.05, 0.10, 0.15) Ferrites. *American Scientific Research Journal for Engineering, Technology, and Sciences* 14(2):72-79.
- Hossain MA, Khan MNI, Sikder SS (2015). "Study of the Variation of Resistivity, Permeability and Curie Temperature of Rare Earth Metal Yttrium (Y) Substitution on $\text{Ni}_{0.60}\text{Zn}_{0.40-x}\text{Y}_x\text{Fe}_2\text{O}_4$ (x=0.05, 0.10, 0.15) Ferrites" *IEEE Xplore, Proceedings of International Conference on Electrical Information and Communication Technology (EICT)*.
- Hossain MA, Khan MNI, Sikder SS (2018). "Complex Permeability and Dielectric Behaviors of Eu^{3+} Doped Ni-Zn Ferrites". *Journal of Asian Scientific Research* pp. 21-29.
- Hussain FI, Najem RA (2018). " La^{+3} Effectiveness Replacement on the Ferrite Material ($\text{Cu}_{0.2}\text{Zn}_{0.45}\text{La}_x\text{Fe}_{2-x}\text{O}_4$) on the Structural and Electrical and Magnetic Features. In *Journal of Physics: Conference Series* 1003(1):012097.
- Qindeela R, Alonizan NH (2018). "Structural, dielectric and magnetic properties of cobalt based spinel ferrites. *Current Applied Physics* 18:519-525.
- Das PS, Singh GP (2016). Structural, magnetic and dielectric study of Cu substituted NiZn ferrite nanorod, *Journal of Magnetism and Magnetic Materials* 401:918-924.
- Heiba ZK, Wahba AM, Mohamed MB (2017). "Structural analysis and magnetic properties of biphasic chromium substituted copper ferrites. *Journal of Molecular Structure* 1147:668-675.
- Ben Tahar L, Artus M, Ammar S, Smiri LS, Herbst F, Vaulay MJ, Richard V, Greneche JM, Villian F, Fievert F (2008). Magnetic Properties of $\text{CoFe}_{1.9}\text{Re}_{0.1}\text{O}_4$ " nanoparticles (RE = La, Ce, Nd, Sm, Eu, Gd, Tb, Ho) prepared in Poyol. *Journal of Magnetism and Magnetic Materials* 323:2420.
- Mansour Al-Haj (2000). Structural Characterization and Magnetization of $\text{Mg}_{0.7}\text{Zn}_{0.3}\text{Sm}_x\text{Fe}_{2-x}\text{O}_4$ Ferrites. *Journal of Magnetism and Magnetic Materials* 299(2):435.
- Gupta N, Kashyap SC, Dube DC (2007). Dielectric and Magnetic properties of Citrate route processed Li-Co Spinel ferrites. *Physica Status Solidi (a)* 204(7).
- Maxwell J (1873). *Electricity and magnetism*. Clarendon. Press Oxford UK.
- Reddy PV, Rao TS (1982). Dielectric behavior of mixed Li-Ni ferrites at low frequencies. *Journal of the Less Common Metals* 86:255-261
- Shrotri JJ, Kulkarni SD, Deshpande CE, Date SK (1999). Effect of Cu substitution on the magnetic and electrical properties of Ni-Zn ferrite synthesized by soft chemical method *Materials Chemistry and Physics* 59(1):1-5.